Evaluation of electric vehicle interior noise focused on sound source identification and transfer path analysis.

D. Fernandez Comesana[1], M. Korbasiewicz[2]

[1] *Microflown Technologies, 6824BV Arnhem, The Netherlands, Email: fernandez@microflown.com*
[2] *Microflown Technologies, 6824BV Arnhem, The Netherlands, Email: korbasiewicz@microflown.com*

Abstract

Vehicles with a fully electric powertrain are becoming more and more popular in the automotive world. The introduction of EV powertrain systems has created a new and significant challenge in the refinement process of vehicles acoustics. The absence of sound masking effects, induced by conventional internal combustion (IC) powertrain, exposes vehicles passengers to a variety of new sound sources. Furthermore, tonal noise created by the motor can become a problem inside the vehicle cabin since it is subjectively more annoying than the broad band noise generated by an IC powertrain. In this paper, an example of an EV car was investigated by employing panel noise contribution analysis (PNCA). PNCA is a well-known methodology for noise quantification and ranking based on airborne Transfer Path Analysis (TPA). The pressure contribution from individual sections of the car interior is calculated by using multiple sound pressure and particle velocity measurements combined with their corresponding airborne transfer paths. PNCA measurements are carried out in real driving conditions with a time stationary excitation (constant speed). The aim of this article is to identify and rank the dominant sound sources perceived from the perspective of the driver of an EV car.

Introduction

One current requirement in the noise, vibration and harshness (NVH) sector is the development of efficient measurement techniques to evaluate the contribution of sound sources to specific locations. A noticeably loud spot in a near-field measurement may have an insignificant contribution to another position outside the measurement plane. This becomes especially critical when assessing vehicles with a fully electric powertrain, where high frequency tones often become the main source of annoyance. Detailed information of the sound propagation paths and the acoustic excitation is required to tackle this problem.

Several pressure contribution techniques, often referred to as "Panel (Noise) Contribution Analysis" methods (PNCA), aim to determine the influence of local excitations upon one reference point in the sound field. In the technical literature, the most commonly used methods are the windowing technique [1], substitution monopole techniques (SMT) [2][3], matrix inversion methods [4], direct particle velocity measurements [5][6], beamforming [7] and acoustic holography [8]. These techniques allow for the areas of local excitation to be ranked; this information is essential for designing effective noise control strategies.

The PNCA method used in this study can be considered an airborne transfer path analysis technique based on measurements of sound pressure and particle velocity [5]. In this paper, the theoretical foundations are derived and the measurement process described. The main investigation focused on the whining noise perceived in an electric vehicle when the car is driven at a constant speed. The evaluation of results and the discussion concentrate on the analysis of the sound pressure contribution maps and the panel raking.

Fundamentals of Panel Noise Contribution Analysis

This section considers the theoretical framework for deriving the fundamentals of PNCA. The following derivation follows Williams [9], although the same expression can also be obtained from the principle of reciprocity, as shown by Hald [8].

The sound pressure p_{ref} located at the reference position $\mathbf{x}$ due to a continuous radiating surface S can be derived from the Kirchhoff-Helmholtz Integral Equation using Green's functions

$$p_{\mathrm{ref}}(\mathbf{x}) = \int_S \left(G(\mathbf{x},\mathbf{y}) \frac{\partial p(\mathbf{y})}{\partial n} - p(\mathbf{y}) \frac{\partial G(\mathbf{x},\mathbf{y})}{\partial n} \right) \mathrm{d}S \qquad \text{[Pa]} \qquad (1)$$

where $p(\mathbf{y})$ is the sound pressure at position $\mathbf{y}$ on the surface S, $\partial/\partial n$ denotes normal derivative on the surface and $G(\mathbf{x},\mathbf{y})$ is the Green function that relates the propagation between the points $\mathbf{x}$ and $\mathbf{y}$. Under free-field conditions, Green's function can be determined via analytical solutions. However, most practical scenarios contain elements that affect sound propagation between the assessed points. Alternatively, Green functions can also be acquired experimentally by measuring the acoustic pressure perceived at a point $\mathbf{x}$ in response to a monopole sound source of controlled source acceleration $\mathrm{j}\omega\rho Q$ located at $\mathbf{y}$, therefore [10]

$$G(\mathbf{x},\mathbf{y}) = \frac{p^{\mathrm{TF}}(\mathbf{x})}{\mathrm{j}\omega\rho Q(\mathbf{y})} \qquad [\mathrm{m}^{-1}] \qquad (2)$$

where $Q(\mathbf{y})$ is the volume velocity of the monopole sound source, ω is the angular frequency, ρ is the density of air and $p^{\mathrm{TF}}(\mathbf{x})$ is the sound pressure measured when a monopole source is exciting the sound field. It should be noted that Eq. 2 implies that a monopole source needs to be positioned at every measurement location $\mathbf{y}$. A reciprocal measurement is often easier to perform. According to the reciprocity theorem, source and receiver can be interchanged, i.e. $G(\mathbf{x},\mathbf{y}) = G(\mathbf{y},\mathbf{x})$, as long as the spatial domain can be considered time-invariant. As a result, the experimental characterization of the Green functions is often performed by placing a monopole source at the reference position $\mathbf{x}$ while measuring near the radiating surface $\mathbf{y}$. Furthermore, Euler's equation of motion makes it possible to obtain an expression for the spatial derivative of the measured Green's function given in Eq. 1 as such

$$\frac{\partial G(\mathbf{y},\mathbf{x})}{\partial n} = \frac{\partial p^{\mathrm{TF}}(\mathbf{y})/\partial n}{\mathrm{j}\omega\rho Q(\mathbf{x})} = \frac{u_n^{\mathrm{TF}}(\mathbf{y})}{Q(\mathbf{x})} \qquad [\mathrm{m}^{-2}] \qquad (3)$$

where $u_n^{\mathrm{TF}}(\mathbf{y})$ represents the acoustic particle velocity measured normal to the surface S when exciting the sound field with a monopole source located at the reference position. The combination of Eq. 1, Eq. 2 and Eq. 3 yields

$$p_{\mathrm{ref}}(\mathbf{x}) = \int_S \left(\frac{p^{\mathrm{TF}}(\mathbf{y})}{Q(\mathbf{x})} u_n(\mathbf{y}) - p(\mathbf{y}) \frac{u_n^{\mathrm{TF}}(\mathbf{y})}{Q(\mathbf{x})} \right) \mathrm{d}S \qquad \text{[Pa]} \qquad (4)$$

It can be shown that the second term of the integral vanishes when data is acquired directly at a rigid boundary [5]. Such an approximation, often referred to as the hard-wall assumption, is used by most pressure-based panel contribution methods. However, in the case that sensors are not directly attached to the surface or the materials are non-rigid, the hard-wall assumption is no longer applicable. The direct acquisition of both sound pressure and particle velocity is then required to avoid large estimation errors at high frequencies, which may become critical in assessing the noise problems of electric vehicles.

For the practical implementation of Eq. 4 it is necessary to subdivide the surface S into N small sections of area ΔS_i. Consequently, Eq. 4 can be written in a discrete form as

$$p_{\mathrm{ref}}(\mathbf{x}) \approx \sum_{i=1}^{N} \left(\frac{p^{\mathrm{TF}}(\mathbf{y}_i)}{Q(\mathbf{x})} u_n(\mathbf{y}_i) - p(\mathbf{y}_i) \frac{u_n^{\mathrm{TF}}(\mathbf{y}_i)}{Q(\mathbf{x})} \right) \Delta S_i \qquad [\mathrm{Pa}] \qquad (5)$$

The above expression enables the reconstruction of the sound pressure p_{ref} at a reference position $\mathbf{x}$ by measuring the sound field at N measurement points. When assessing the noise radiated by a complex structure, such as a vehicle cabin interior, it is convenient to study the contribution of the different constructive elements using several measurement positions. This implies that K probes are grouped in order to calculate the partial contribution of each element. Assuming that an area of equal size is associated with each probe, we can formulate an expression in terms of the spatially averaged contribution per unit area $\langle p_{\mathrm{cont}} \rangle$ and the total panel area A_P, i.e.

$$\hat{p}_{\mathrm{cont}} = A_P \langle p_{\mathrm{cont}} \rangle = A_P \, \frac{1}{K} \sum_{i=1}^{K} \left(\frac{p^{\mathrm{TF}}(\mathbf{y}_i)}{Q(\mathbf{x})} u_n(\mathbf{y}_i) - p(\mathbf{y}_i) \frac{u_n^{\mathrm{TF}}(\mathbf{y}_i)}{Q(\mathbf{x})} \right) \qquad [\mathrm{Pa}] \qquad (6)$$

The general definition shown in Eq. 5 implies that the entire distribution of sound pressure and normal particle velocity should be acquired simultaneously in order to accurately reconstruct the reference pressure. This condition may become critical at low frequencies, due to the presence of few dominant correlated, or partially-correlated, sources in the entire cabin interior. In order to overcome this problem, several methods, such as the "Reference-Related method"[11] have been proposed in the literature. However, the noise assessment for most electric vehicles is mainly focused on high frequencies where the size, damping, and modal density of the vehicle allow phase information between constructive elements to be disregarded [12]. Consequently, the sound pressure reference can be synthesized in terms of squared amplitude using the summation of M individual contributions as

$$|p_{\mathrm{ref}}(\mathbf{x})|^2 \approx \sum_{i=1}^{M} |\hat{p}_{\mathrm{cont},i}|^2 \qquad [\mathrm{Pa}^2] \quad (7)$$

Measurement methodology

The input datasets required for PNCA are determined via two independent measurement steps. Firstly, the acquisition of the acoustic excitation is performed in operational conditions while the array is attached to a car section. Secondly, the characterisation of the sound propagation is performed by introducing a monopole sound source at the reference location whilst the vehicle is static. Figure 1 illustrates this measurement procedure.

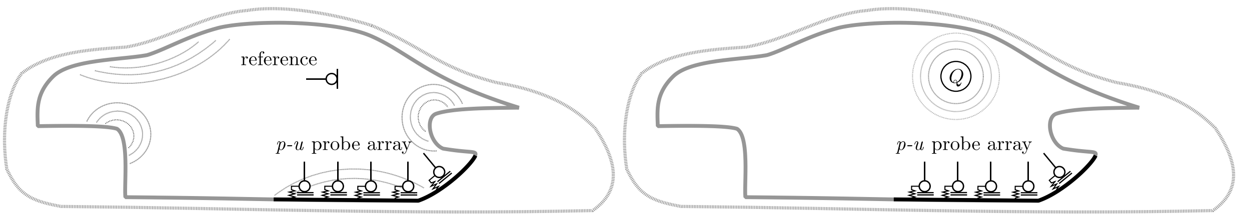

Figure 1: Sketch of the two measurement stages: operational (left) and transfer path (right) measurement steps of a car section.

In this paper, measurements were performed in a Renault ZOE. Operational data was acquired whilst driving at a constant speed of 40 km/h on the highway. A preliminary investigation was undertaken by listening to normal particle velocity while manually moving a *p-u* probe across the cabin interior. This initial step helped to identify key spots that should be covered by probe locations. An array of 11 *p-u* intensity probes was attached to several car sections using spring mountings to decouple sensors from surface vibrations. The probe array was re-positioned 16 times, ensuring the cabin surface was completely covered with a total of 176 measurement points. Figure 2 shows a picture of the measurement setup for one of the assessed sections along with the source used as excitation during the transfer path measurements.

Figure 2: Pictures of the sensor attached to the front passenger door (left) and monopole source used for transfer path measurements (right).

A random incidence microphone was fixed at the driver's seat to measure the reference sound pressure perceived by the driver during each session. Figure 3 shows the sound pressure levels recorded during the different sessions. As can be seen, the variance is relatively low, making it possible to compare data acquired during separate measurement sessions.

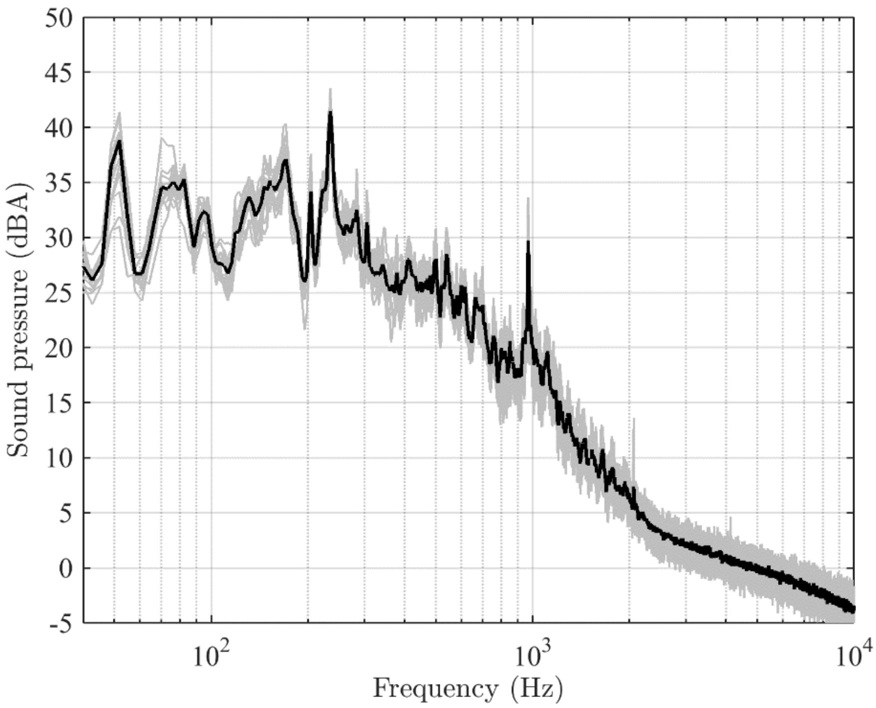

Figure 3: Sound pressure spectra of each individual session (grey lines) and averaged (black line) recorded at the reference position.

Analysis of results

The acquisition of data using a sound intensity *p-u* probe array with the PNCA methodology provides detailed information about not only the vibrating structure under assessment but also the acoustic environment. Normal particle velocity maps can be used to study the excitation distribution regardless of the frequency range of interest [11]. On the other hand, the transfer function acquired could reveal amplification, or attenuation effects caused by the geometry and properties of the cabin interior. For the sake of brevity, this paper focuses on source localization and pressure contribution quantification in potentially problematic spectral regions. Therefore, the strong tonal component that can be seen in the reference spectrum, shown above at 970 Hz, is of special interest. It represents one of the most common problems of current electric vehicles: high frequency whistling noise known as *whining*. As such, this section focuses on finding, quantifying and ranking the main car sections that induce this noise.

Source localization

One of the main challenges in cabin interior noise optimization is how to identify the areas of the structure that produce significant acoustic excitation, i.e. the localisation of the main noise sources. The high complexity of a car interior requires efficient ways to visualize the large amount of data gathered. First of all, Figure 4 shows the particle velocity spectra of all measured car sections in the frequency range of interest. This graph indicates that the car sections with a significant excitation are mainly located within the front part of the vehicle.

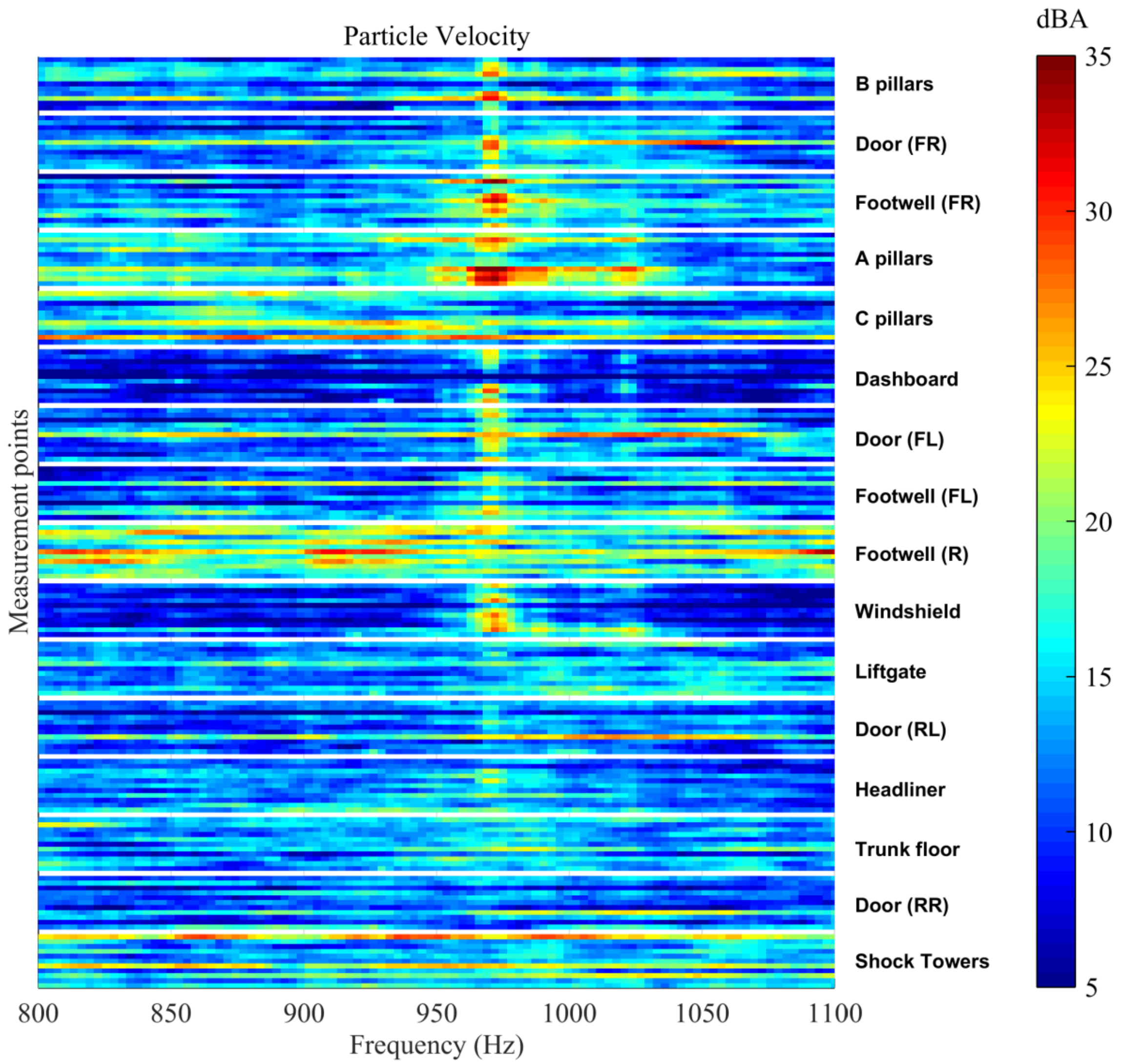

Figure 4: Acoustic particle velocity of all measured probe positions.

There are several car sections that have significantly high excitation, although it is not yet clear which part of the constructive element is problematic. In order to get a better understanding of the spatial distribution within each panel, Figure 5 presents particle velocity colormaps of the most relevant areas at 970 Hz.

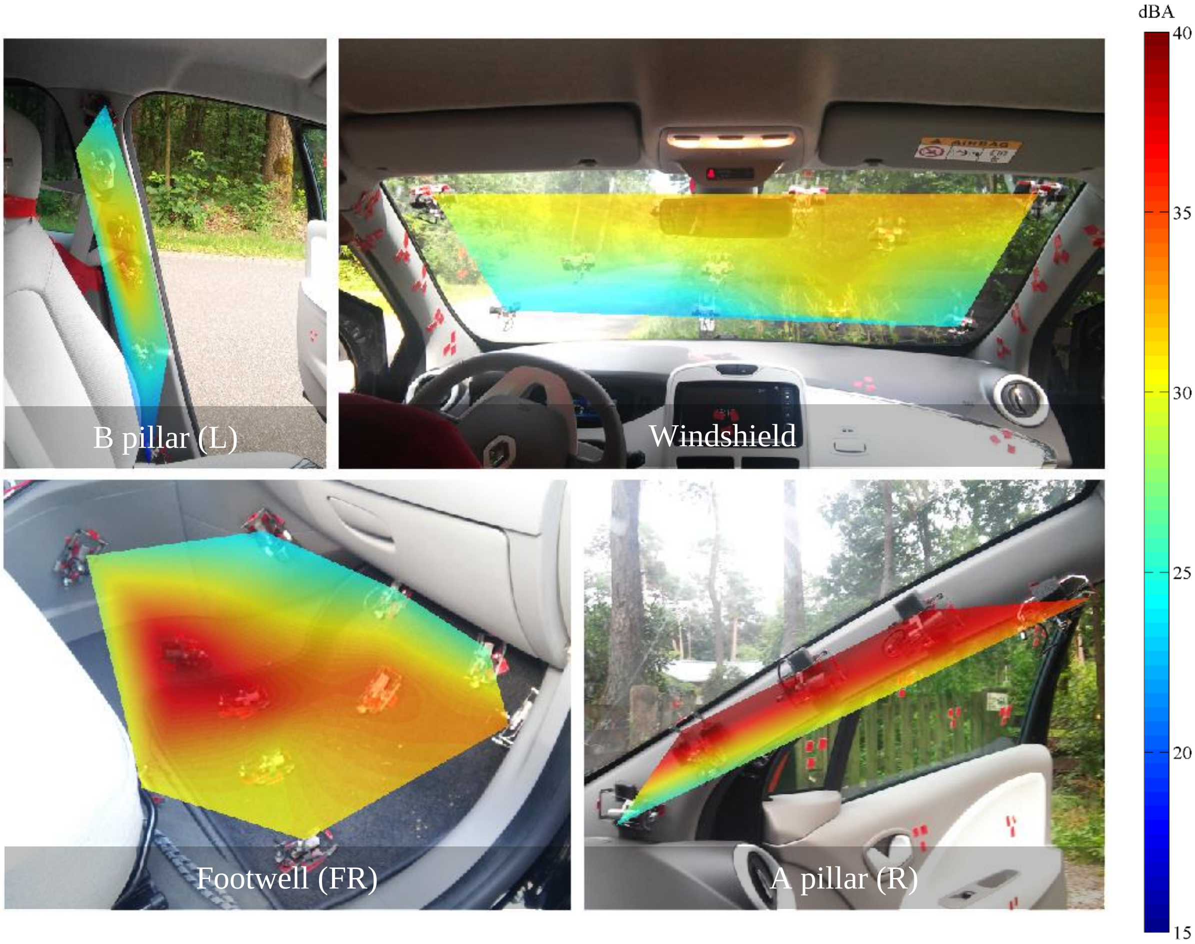

Figure 5: Particle velocity distribution of some relevant car sections at 970 Hz.

As shown, the highest levels are perceived at the A pillars. Poor sealing between the plastic cover and the main structure could be transmitting noise into the cabin interior. Furthermore, a strong weakness was detected on the B pillar at the seatbelt insertion point. Other panels, such as the windshield or front footwell, could also have a significant impact on the sound pressure perceived at the driver's ear.

Panel quantification and ranking

Measurements of normal particle velocity provide useful information about the acoustic excitation produced by the different radiating surfaces in operational conditions. However, the computation of the contribution of a particular element combines both sound pressure and particle velocity measurements with their corresponding sound propagation paths. Recalling Eq. 6, it is also required to define the surface area of the assessed elements. As shown below, the wrong definition of this factor may cause significant bias in the source ranking. In this paper, a 3D scanner known as a *structure sensor* [13] was used to acquire the areas of the different car sections. This sensor makes it possible to create a 3D model of the car interior in a matter of minutes by manually moving the sensor across the vehicle. Figure 6 shows a sample of the model created together with the panel areas calculated.

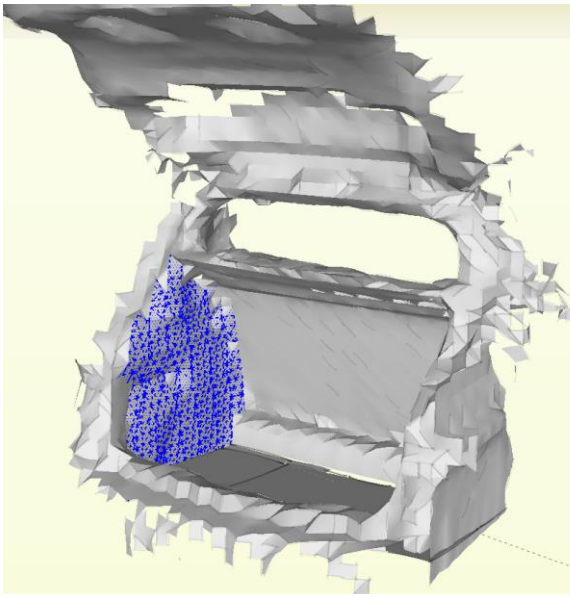

Section	Area (m^2)	
Windshield	1	
Dashboard	1	
Footwell (F R)	1.2	0.5
Ceiling	1.8	
Door (FL FR; RL RR)	0.6	0.6
	0.6	0.6
A pillar (L R)	0.15	0.15
B pillar (L R)	0.25	0.25
C pillar (L R)	0.2	0.2
Shock towers (RL RR)	0.35	0.35
Trunk floor	0.6	
Liftgate	1.25	

Figure 6: Sample of the 3D model used to calculate section areas (left) and results obtained (right).

The pressure contribution results obtained for the most relevant sections are shown in Figure 7 before (light grey) and after (dark grey) incorporating the area into the contribution calculations. As can be seen, the whining noise perceived by the driver is mainly caused by the A-pillars, which is in line with the source localization results shown above. It should be noted that the area of the panel acts as a weighting factor which greatly affect the results when the element has an area that differs notably from unity. The significant differences between this contribution and the rest, suggest that the application of acoustic treatment to these pillars could result in a substantial reduction of the whining noise perceived at the reference position.

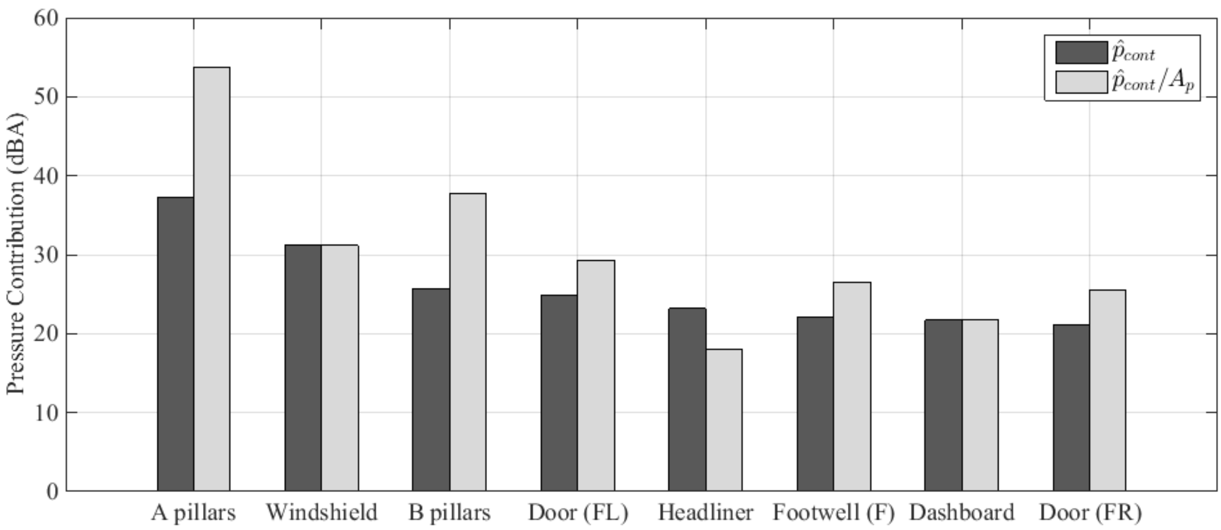

Figure 7: Source ranking of the main car sections focused on the whining noise at 970 Hz.

Conclusions

A measurement technique suitable for performing panel contribution analysis has been applied to address one of the main problems associated with most electric vehicles: whining noise. The theoretical foundations of the measurement method have been reviewed in detail, emphasizing the importance of the assumptions made in the derivation concerning high frequency noise. A practical case, a full car interior, has been evaluated using the presented measurement methodology. Particle velocity measurements acquired near the different car surfaces were proven to localize the sections of the cabin interior that induce a high excitation. The impact of including the surface area into the contribution calculation has been assessed, demonstrating that this factor becomes critical when comparing car interior construction elements of different sizes. Finally, a ranking of the main sections of the car interior was presented, showing that the A-pillars were the dominant excitation in the case studied. This information could potentially be used to apply acoustic treatments to the problematic element in order to reduce the noise perceived at a specific location.

References

[1] S. Sorenson, "Investigation of different techniques for quantifying automotive panel noise radiation," in SAE Technical Paper 951267, 1995.

[2] J. Rondeau, A. Duval, G. Deshayes, M. Lassalas, H.-E. de Bree, and S. Chaigne, "Vehicle acoustic synthesis method: Improving acquisition time by using p-u probes," in SAE Technical Paper 2005-01-2444, 2005.

[3] J. W. Verheij, "Inverse and reciprocity methods for machinery noise source characterization and sound path quantification," International Journal of Acoustics and Vibration, vol. 2(1), pp. 11-20, 1997.

[4] LMS, "Transfer Path Analysis, the qualification and quantification of vibroacoustic transfer paths," LMS International, Application Notes, 2005.

[5] O. Wolff , "Fast panel noise contribution analysis using large PU sensor arrays," in Proceedings of Internoise, 2007.

[6] C. Bertolini, J. Horak, M. Mantovani, and G. L. Sinno, "Interior panel contribution based on pressure-velocity mapping and acoustic transfer functions combined with the simulation of the sound package," in Proceedings of Internoise, 2011.

[7] C. Cariou, O. Delverdier, S. Paillasseur and L. Lamotte, "Tool for interior noise sources detection in aircraft with comparison of configurations," in Berlin Beamforming Conference, 2012.

[8] J. Hald, M. Tsuchiya, C. Blaabjerg, H. Ando, T. Yamashita, M. Kimura and Y. Ishii, "Panel contribution analysis using a volume velocity source and a double layer array with the SONAH algorithm. In InterNoise and NoiseCon Congress and Conference Proceedings, vol. 2006, no. 6, pp. 1465-1474, Institute of Noise Control Engineering, 2006.

[9] E. G. Williams, "Fourier Acoustics: Sound Radiation and Nearfield Acoustical Holography," Academic Press, 1999.

[10] K. R. Holland and P. A. Nelson, "The application of inverse methods to spatially-distributed acoustic sources," Journal of Sound and Vibration, 332, (22), 5727-5747, 2013.

[11] D. Fernandez Comesana: "Scan-based Sound Visualisation Methods using Sound Pressure and Particle Velocity," University of Southampton, Institute of Sound and Vibration Research, Doctoral Thesis, 2014.

[12] C.T. Musser, J. E. Manning, and G. Chaoying Peng. "Predicting Vehicle Interior Sound with Statistical Energy Analysis." Sound and Vibration, December 2012.

[13] Occipital, Inc. "The structure sensor", http://www.structure.io/, 2008 (accessed 11 September 2015).